Impaired Lung Homeostasis in Neonatal Mice Exposed to Cigarette Smoke

Sharon McGrath-Morrow[1], Tirumalai Rangasamy[2], Cecilia Cho[1], Thomas Sussan[2], Enid Neptune[3], Robert Wise[3], Rubin M. Tuder[4], and Shyam Biswal[2,3]

[1]Department of Pediatrics; [2]Department of Environmental Health Sciences, Bloomberg School of Public Health; [3]Department of Medicine, Division of Pulmonary and Critical Care Medicine; and [4]Department of Pathology, Division of Cardiopulmonary Pathology, The Johns Hopkins Medical Institutes, Baltimore, Maryland

In infants, smoke exposure is associated with more respiratory illnesses and decreased lung function. We hypothesized that perinatal lung is particularly susceptible to the damaging effects of cigarette smoke (CS) and that exposure to CS during this period may alter expression of immune response genes and adversely affect lung growth. To test this, we exposed neonatal mice to 14 days of CS. Immediately after exposure to CS, pulmonary gene expression profiling was performed on 2-week-old CS-exposed lung and age-matched control lung. Nitrotyrosine, TUNEL, MAC3, and phospho-SMAD-2 (p-SMAD2) staining was also performed. At 8 weeks of age, lung volume measurements were determined and mean linear intercept measurements were calculated. Pulmonary gene expression profiling revealed that CS exposure significantly inhibited type 1 and type 2 interferon pathway genes in neonatal lung, compared with age-matched control lung. Neonatal CS-exposed lung also had a significant increase in n-tyrosine, TUNEL, and p-SMAD2 staining when compared with adult CS-exposed lung and age-matched control lung. Lung volumes at 8 weeks of age were modestly but significantly decreased in mice exposed to CS in the neonatal period compared with age-matched controls, consistent with impaired lung growth. The results of this study indicate that exposure to CS during the neonatal period inhibits expression of genes involved in innate immunity and mildly impairs postnatal lung growth. These findings may in part explain the increased incidence of respiratory symptoms in infants and children exposed to CS.

Keywords: neonatal lung; cigarette smoke; interferon responsive genes; oxidative stress; TGF-β signaling

Cigarette smoke (CS) exposure has a significant impact on the respiratory health of infants and children (1). Infants exposed to CS are at higher risk for sudden infant death syndrome, lower respiratory tract infections, and small airway disease, compared with infants not exposed to CS (2–4).

We hypothesize that perinatal life represents a period of critical vulnerability in which exposure to CS may impair lung immunity and lung growth. The innate immune system of the neonate is immature, which may account for the increased susceptibility of infants to viral and bacterial pathogens (5). Exposure to CS during perinatal life may further depress the innate immune system in the lung. *In vitro* studies have shown that CS extract inhibits TH1 cytokines, such as IL-1β, IL-2, IFN-γ, and TNF-α (6), and macrophages exposed to CS have an

CLINICAL RELEVANCE

In our study cigarette smoke inhibited innate gene expression and led to a modest impairment of alveolar growth. These results may help explain the increased incidence of respiratory symptoms in infants exposed to tobacco smoke.

impaired IFN-γ response (7). Furthermore, in one of the few studies evaluating the effect of CS on the neonatal immune system, investigators found that neonatal mice exposed to both CS and respiratory syncytial virus (RSV) had lower levels of TH1 cytokines in the bronchoalveolar lavage fluid compared with control mice exposed to RSV alone (8).

Another concern with regard to perinatal life and CS is the effect of CS exposure on postnatal alveolar growth. During the perinatal period, the lung continues to develop new alveoli. This occurs in both the human and rodent lung (9). In the rodent, most growth occurs during the first 2 weeks of postnatal life, while alveolar growth in the human extends to about the first 2 years of life (10). We and others have shown that mice exposed to hyperoxia during the perinatal period have impaired alveolar growth, leading to abnormalities in lung structure and function that persist into adult life (11–13). Children are at risk for adverse pulmonary effects when exposed to environmental pollutants. A recent study found that children living close to highways and exposed to high levels of pollutants have significantly lower lung function than children who live at further distances from the highway (14). CS has over 4,500 chemicals in the form of particles and gases that include carcinogens and reactive aldehydes (3, 15). Exposure to these chemicals in early life may adversely effect postnatal lung growth and immune function. Although exposure to CS is ubiquitous in most areas of the world, little is known regarding the effects of CS on postnatal lung growth.

We hypothesized that CS exposure interferes with neonatal lung homeostasis by inhibiting expression of pulmonary immune-response genes and impairing lung growth. To study the effects of CS exposure on neonatal lung, we exposed neonatal mice to CS for the first 2 weeks of life. The daily exposure of neonates to CS was limited and significantly less than that which had previously been used to induce emphysema in the adult mouse (16).

MATERIALS AND METHODS

C57BL/6J mice were procured from The Jackson Laboratory (Bar Harbor, ME). The animals were maintained on an AIN 76A diet and water *ad libitum* and housed at a temperature range of 20 to 23°C under 12-hour light/dark cycles.

All experiments were conducted in accordance with the standards established by the United States Animal Welfare Acts, set forth in NIH guidelines and the Policy and Procedures Manual of the Johns Hopkins University Animal Care and Use Committee. C57BL/6J mice were used for all experiments.

CS Exposure

The smoke machine (Model TE-10; Teague Enterprises, Davis, CA) was adjusted to burn two cigarettes (2R4F reference cigarettes, 2.45 mg nicotine/cigarette; purchased from the Tobacco Health Research Institute, University of Kentucky, Lexington, KY) at one time. Cigarettes were smoked with standard puffs of 35 ml volume of 2-second duration. The total particulate matter in the exposure chambers was on an average 90 mg/m^3, and CO concentration was 350 ppm (16). Mice were divided into the following four groups: 1-day-old mice with their mothers and 6-week-old adult mice were placed in the smoke chamber for 1 hour/day during the first week and 2 hours/day during the second week of exposure. As controls, 1-day-old mice and 6-week-old mice were kept in a filtered air environment away from the experimental groups.

Mice exposed to 2 weeks of CS as neonates were killed at either 2 or 8 weeks of age, 6-week-old mice exposed to 2 weeks of CS were killed at 8 weeks of age, and control mice kept in the filtered air environment were killed at either 2 or 8 weeks of age.

Lung Processing

Lungs were infused through the trachea with 0.5% low-melting agarose using a fixed volume. Lungs were fixed overnight in 10% buffered formalin and then paraffin-embedded. Lung was cut into 5-μm lung sections.

Immunocytochemistry

For immunohistochemistry, antigen retrieval was performed using citrate buffer for 30 minutes, then washed. Slides were blocked with 3% H$_2$O$_2$ for 15 minutes. Lectin (Bioinylated GSL I-isolectin B4, #B-1205; Vector Laboratories, Burlingame, CA) and anti-mouse MAC3 rat monoclonal antibody (#550292; BD Pharmingen, San Diego, CA) were used to identify macrophages in lung sections. For quantification of cell proliferation, rabbit anti-proliferating cell nuclear antigen (PCNA) was used as the primary antibody (#SC-7907, 1:50 dilution; Santa Cruz, Santa Cruz, CA) for 1 hour, washed, and the second antibody, goat anti-rabbit Texas Red (#T2767, 1:200; Molecular Probes, Eugene, OR) was applied for 20 minutes. The following primary antibodies were used in separate reactions: pSMAD2 (#3101, 1:1,000 dilution; Cell Signaling, Danvers, MA) and active caspase 3 rabbit polyclonal antibody (10 μg/ml, ab2302; Abcam, Cambridge, MA). Primary antibodies were applied for 1 hour at room temperature then washed. Secondary antibody, using Envision+System HRP (# K4010; DakoCytomation) was applied for 1 hour at room temperature and developed with diaminobenzidine (DAB) (#K3468; DakoCytomation), counterstained, dehydrated, and mounted with permount. For illustration purposes the fluorescent secondary antibody Streptavidin Texas Red conjugate (dilution 1:200, S/872; Molecular Probes) was also used after administration of primary pSMAD2 antibody (Figure 1A). For quantification of oxidative stress, rabbit polyclonal anti-nitrotyrosine antibody (Upstate, Lake Placid, NY) and secondary rabbit-HRP conjugate (DakoCytomation) were used with

DAB as the substrate. Positive staining cells that were developed by DAB were quantified using Metamorph software (Molecular Devices Corp., Downingtown, PA) and normalized to lung perimeter. Ten random sections from each slide were acquired with a ×10 lens by an observer masked to the identity of the experimental group.

Cell death was quantified using Fluorescein-FragEL DNA Fragmentation Detection Kit (Oncogene, Boston, MA). The lung sections were stained with TdT labeling reaction mixture and mounted using Fluorescein-FragEL mounting medium. DAPI and fluorescein were visualized at 330 to 380 nm and 465 to 495 nm, respectively. Images of the lung sections (15/lung section) were captured using Nikon Eclipse E800 microscope (Nikon, Melville, NY) with a ×20 lens. DAPI-positive cells (blue) and apoptotic cells (green) were counted, by an observer, blinded to the identity of the slides. Apoptotic cells were normalized to the total number of DAPI-positive cells.

Lung Morphometry

Lung sections were stained with hematoxylin and eosin. Mean linear intercept (MLI), alveolar number, and alveolar radius were measured using macro processing developed with the Metamorph software (Molecular Devices) and recorded as arbitrary units, as previously described (11). Each slide contained tissue from the left lobe and represented an individual animal. Ten random sections from each slide were acquired with a ×10 lens by an observer masked to the identity of the experimental group. Large airways and vessels were avoided. The MLI was determined using the average distance between intersects of approximately 40 lines interposed to the image.

Water Displacement Method

Eight-week-old mice were killed and lungs were inflated at 20 cm H$_2$O with 0.5% agarose, then removed from the thorax. Extrapulmonary tissues were carefully removed and the total lung volume was determined by the water displacement method according to Scherle (17).

Gene Expression Profiling

Total RNA was extracted from lung of 2-week-old mice exposed to 14 days of CS ($n = 6$) and from lung of 2-week-old control mice ($n = 4$) using TRIzol reagent and purified using RNAeasy mini kits (Qiagen, Valencia, CA). Purified total RNA was reverse transcribed to first-strand cDNA using a hybrid primer consisting of oligo-dT and T7 RNA polymerase promoter sequences. The single-stranded cDNA was then converted to double-stranded cDNA. Complementary DNA corresponding to 5 to 10 μg of total RNA was used in a cRNA amplification step using T7 RNA polymerase and a biotinylated nucleotide precursor. The resulting biotinylated cRNA was fragmented to a size of approximately 50 bp. Approximately 20 to 30 μg of cRNA from each tissue was hybridized to corresponding (Mouse Genome 430 2.0 Array) GeneChips (Affymetrix, Santa Clara, CA). The bound cRNA was visualized by binding of streptavidin/phycoerythrin conjugates to the hybridized GeneChip, followed by laser scanning of bound phycoerythrin. The differentially
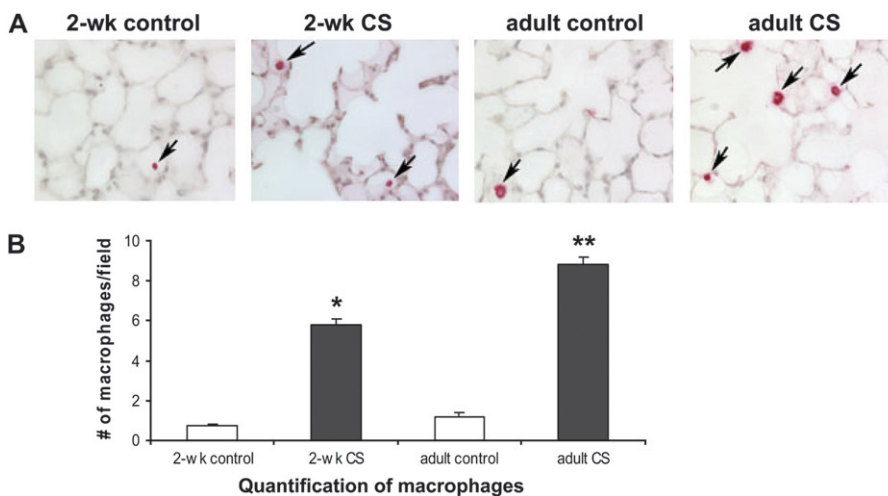
Figure 1. Increased alveolar macrophages in cigarette smoke (CS)-exposed mice. (*A*) Increased numbers of alveolar macrophages were found in both 2-week-old and adult mice exposed to 14 days of CS (*black arrows* point to macrophages). (*B*) Significantly more alveolar macrophages by MAC3 staining per field was found in 2-week-old and adult CS-exposed mice compared with age-matched controls (**P < 0.001 by one-way ANOVA). Increased macrophage staining per field was found in adult CS-exposed mice compared with 2-week-old CS-exposed, 2-week-old control, and adult control mice (***P < 0.001 by one-way ANOVA, n = 3 for all groups, ± SEM).

expressed transcripts were analyzed using pairwise comparison with Data Mining Tool 3.0 program (Affymetrix). Only those differentially expressed genes that appeared in at least six of the nine comparisons and showed a change of more than 1.5-fold were selected. Mann-Whitney pairwise comparison test was performed to rank the results by concordance as an indication of the significance ($P < 0.05$) of each identified change in gene expression. Entire profiling results can be accessed through the website, geo@ncbi.nlm.nih.gov, using accession number GSE7310.

Quantitative RT-PCR Analysis

Reverse transcription was performed using total RNA isolated from CS-exposed and control 2-week-old mouse lung and processed with the SuperScript first-strand synthesis system for RT-PCR according to the manufacturer's protocol (Invitrogen, Carlsbad, CA). QRT-PCR was performed using the Applied Biosystems (Foster City, CA)TaqMan assay system. All PCR amplifications were carried out on an ABI Prism 7700 Sequence Detection System, using a fluorogenic 5′ nuclease assay (TaqMan probes). Probes and primers were designed and synthesized by Applied Biosystems. Relative gene expressions were calculated by using the 2^{-Ct} method, in which Ct indicates cycle threshold, the fractional cycle number where the fluorescent signal reaches detection threshold. The normalized ÿCt value of each sample was calculated using the mouse GADPH gene as an internal endogenous control. The data were analyzed using the Sequence Detector Software SDS 2.0 (Applied Biosystems). PCR reaction of each sample was run in triplicates.

Statistics

Statistical calculations were performed for gene expression profiling and real-time PCR as described above. Differences in measured variables between experimental groups and control groups were determined using nonparametric Wilcoxon rank sum test, one-way ANOVA, and Student's *t* test (two-tailed, equal variance) using the SPSS 14 statistical software (Chicago, IL). Statistical significance was accepted at $P < 0.05$.

RESULTS

Down-Regulation of Immune Response Genes in CS-Exposed Neonatal Lung

Gene expression profiling was used to identify genes differentially regulated in lungs of 2-week-old mice exposed to CS. Mouse Genome 430 2.0 Array Affymetrix Gene Chips were used for profiling and analysis (CS-exposed lung, $n = 6$; age-matched control lung, $n = 4$). CS exposure induced the expression of 196 genes and inhibited the expression of 754 genes. Approximately 10% of the down-regulated genes were type 1 (α/β) and type 2 (γ) interferon (IFN) response genes, genes shown to be integral to the innate immune response (18).

CS Inhibited Interferon-Inducible GTPase Expression in Neonatal Lung

CS exposure was found to inhibit gene expression of four interferon-inducible GTPase families. These included p47, p65 guanylate binding protein (GBP), myxovirus (MX), and very large inducible GTPases (VLIG) (Table 1). Interferon-inducible GTPase-1 (IIGP1), a p47 GTPase induced in response to intracellular protozoa (19), underwent a −9.71-fold change by microarray analysis. Validation by QRT-PCR revealed a 6.3-fold decrease in IIGP1 in 2-week-old CS-exposed lung compared to age-matched control lung ($P < 0.0001$).

CS Inhibited Expression of Genes Activated by Double-Stranded (ds) RNA in Neonatal Lung

Viral double-stranded (ds) RNA activates the innate immune system by inducing type 1 IFN response genes. Gene expression profiling from 2-week-old CS-exposed lung revealed significant inhibition of several type 1 IFN response pathway genes induced by viral dsRNA (Table 2). Toll-like receptor 3 (TLR-3), a pattern

TABLE 1. NEONATAL CS INHIBITS INTERFERON-INDUCIBLE GTPase GENES

	Gene Symbol	Fold Change	P Value
p47 GTPases			
Interferon-inducible GTPase-1	IIGP1	−9.71	0.005
Interferon-inducile GTPase-2	IIGP2	−6.77	0.005
Interferon-γ–induced GTPase	IGTP	−7.52	0.005
Interferon inducible protein 1	LRG-47/ IFI1	−5.94	0.005
Interferon gamma inducible protein 47	IRG-47/ IFI47	−5.74	0.005
T cell–specific GTPase	TGTP	−6.68	0.005
VLIG GTPases-secondary response			
GTPase, very large interferon inducible 1	GVIN1	−5.03	0.005
p65 GBP GTPase			
Guanylate nucleotide binding protein 2	GBP2	−5.17	0.005
Guanylate nucleotide binding protein 4	GBP4	−5.9	0.005
Mx GTPases			
Myxovirus resistance 1	MX1	−5.5	0.005
Myxovirus resistance 2	MX2	−19.56	0.005

recognition receptor for dsRNA (20), was significantly decreased (−3.4) and expression of interferon regulatory factor 7 (IRF7) a transcription factor central to the initiation of type 1 IFN immune responses (21) and downstream of TLR-3 was also inhibited (−2.66) in CS-exposed lung. Other pathways induced by type 1 IFN responses but independent of TLRs were also suppressed. Both retinoic acid–inducible protein 1 (RIG-1) and melanoma differentiation associated gene 5 (MDA5) were inhibited in CS-exposed lung (−2.43 and −4.08, respectively). These genes contain DexD/Hbox RNA helicases that interact with dsRNA and are critical for host recognition of specific RNA viruses (22). CS exposure also caused down-regulation of several genes that when activated by dsRNA can inhibit viral protein translation. IFN-type 1–induced and dsRNA-activated kinase (PKR) underwent a −6.54-fold change in the CS-exposed lung. Activation of PKR by dsRNA leads to phosphorylation of the α subunit of eukaryotic translation initiation factor 2 (eIF2α) and phosphorylation of eIF2α blocks viral protein synthesis (23). Interferon-induced protein with tetratricopeptide repeats 1 (IFIT1/p56), a protein that inhibits viral protein translation by

TABLE 2. NEONATAL CS INHIBITS GENES ACTIVATED BY VIRAL DOUBLE-STRANDED RNA

	Gene Symbol	Fold Change	P Value
Activated by viral double-stranded RNA/induces type 1 IFN response			
Toll-like receptor 3	TLR-3	−3.4	0.005
Retinoic –acid–inducible protein 1	RIG-1	−2.43	0.005
Fas death domain–associated protein	DAXX	−1.88	0.005
Melanoma differentiation associated gene 5	MDA5	−4.08	0.005
DNA segment, Chr 11, Lothar Hennighausen 2, expressed	LGP2e	−11.63	0.005
Interferon regulatory factor 7	IRF-7	−2.66	0.005
Inhibits initiation of translation			
Interferon type I–induced and double-stranded RNA-activated kinase	PKR	−6.54	0.005
Interferon-induced protein with tetratricopeptide repeats 1	IFIT1/p56	−19.84	0.005
Interferon-induced protein with tetratricopeptide repeats 2	IFIT2	−4.69	0.005
Interferon-induced protein with tetratricopeptide repeats 3	IFIT3	−13.74	0.005
2′-5′ oligoadenylate synthetase-like 2	OASL2	−6.15	0.005
2′-5′ oligoadenylate synthetase-like1	OASL1	−3.16	0.005
2′-5′ oligoadenylate synthetase-1A	OASLA	−4.79	0.005
Adenosine deaminase RNA specific	ADAR	−5.5	0.005
Z-DNA–binding protein 1	ZBP1	−12.47	0.005

TABLE 3. NEONATAL CS INHIBITS SMALL INTERFERON–STIMULATED GENES

	Gene Symbol	Fold Change	P Value
Ubiquitin-like proteins-activated by type 1 IFNs			
Interferon, alpha-inducible protein	ISG15/Glp2	−6.92	0.005
Interferon, alpha-inducible protein 27	ISG12/IFI27	−7.11	0.005
Interferon-stimulated protein	ISG20	−2.31	0.005
ISG15 conjugation			
Ubiquitin-activating enzyme E1-like	UBE1L	−2.39	0.005
Hect domain and RLD 5 (E3 enzyme)	HERC5	−5.7	0.005
ISG15 deconjugating protease			
Ubiquitin specific protease 18	USP18/UBP43	−8.57	0.005

interfering with eIF3, underwent a −19.84 fold-change (24). Microarray results also revealed down-regulation of several 2′-5′oligoadenylate synthetase genes, genes that inhibit protein synthesis by activating Rnase L (OASL1, OASL2, OASLA, −3.16, −6.15, and −4.79, respectively) (25). Both PKR and the OAS/Rnase L genes are important for host defense against coxsackievirus infection (26). Two other IFN-inducible genes down-regulated by CS included the dsRNA editing enzyme, adenosine deaminase, RNA-specific (ADAR) and Z-DNA–binding protein 1 (ZBP1) (−5.5 and −12.47, respectively), both of which contain Z-DNA binding domains that bind dsRNA in a left-handed Z conformation (23).

CS Inhibited Expression of Small Interferon–Stimulated Genes (ISGs) in Neonatal Lung

ISG15 is a ubiquitin-like gene, induced by type 1 IFNs α/β and conjugated by ubiquitin-activating enzyme E1-like (UBE1L), UBCH8 (E2 enzyme), and Hect domain and RLD 5 (HERC5, an E3 enzyme) to induce genes necessary for anti-viral defense (27, 28). We found that expression of ISG15, UBE1L, and HERC5 was significantly decreased in CS-exposed lung (−6.95, −2.39, and −5.7, respectively) (Table 3). The small intracellular nonsecreted IFN-regulated gene, ISG12, shown to protect neonatal mice against viral encephalitis, was also inhibited in CS-exposed lung (−7.11) (29).

CS Increased Alveolar Macrophages in 2-Week-Old and 8-Week-Old Mice

MAC3 staining was used to quantify alveolar macrophages in lung from 2-week-old CS-exposed mice and age-matched con-

trols. MAC3 staining was also performed in adult mice, exposed to 2 weeks of CS as adults and age-matched controls. We found significantly more MAC3 staining in lung of CS-exposed 2-week-old and adult mice compared with age-matched controls (Figure 1, $P < 0.001$, respectively). Interestingly, when adult mice were exposed to 14 days of CS, they had significantly more alveolar macrophages then neonatal mice exposed to 14 days of CS ($P < 0.001$).

CS Increased Oxidative Stress and Cell Death in Neonatal Lung

Nitrotyrosine (n-tyrosine) staining was used to quantify oxidative stress in the lung of mice exposed to CS. CS exposure led to an increase in n-tyrosine staining in the 2-week-old mice compared with age-matched control lung (Figure 2, $P < 0.03$ by Wilcoxon ranksum test). There was no increase in n-tyrosine staining in lung from mice exposed to 14 days of CS as adults. This finding suggests that neonatal lung may be more sensitive to the effects of CS then adult lung.

To determine if CS exposure induced a change in pulmonary cell proliferation, PCNA staining (a marker of cell proliferation) was performed on murine lung. There was no difference in PCNA staining between 2-week-old CS-exposed and age-matched control lung detected. TUNEL staining, however, was increased in the lung of 2-week-old mice exposed to CS compared with age-matched control lung (Figure 3, $P < 0.0001$). We also found an increase in TUNEL staining in lung of mice exposed to CS as adults compared with age-matched control mice ($P < 0.001$). The number of TUNEL-positive lung cells in the adult CS-exposed mice, however, was significantly less than that found in 2-week-old CS-exposed mice ($P < 0.001$). These findings demonstrate that CS exposure during the perinatal period increases pulmonary cell death to a greater degree then that found in adult mice exposed to similar amounts of CS. To determine if TUNEL staining was representative of apoptotic or necrotic cell death, caspase 3 staining was performed. No difference in caspase 3 staining was found in lung from 2-week-old CS-exposed mice and age-matched controls, indicating that CS exposure caused necrotic cell death in lung of neonatal mice exposed to CS.

Up-Regulation of TGF-β2 and TGF-β Signaling in Neonatal CS-Exposed Lung

Gene expression profiling revealed significant up-regulation of the TGF-β2 gene in neonatal lung exposed to CS (+1.79, $P < 0.005$). Induction of TGF-β had been shown to be associated
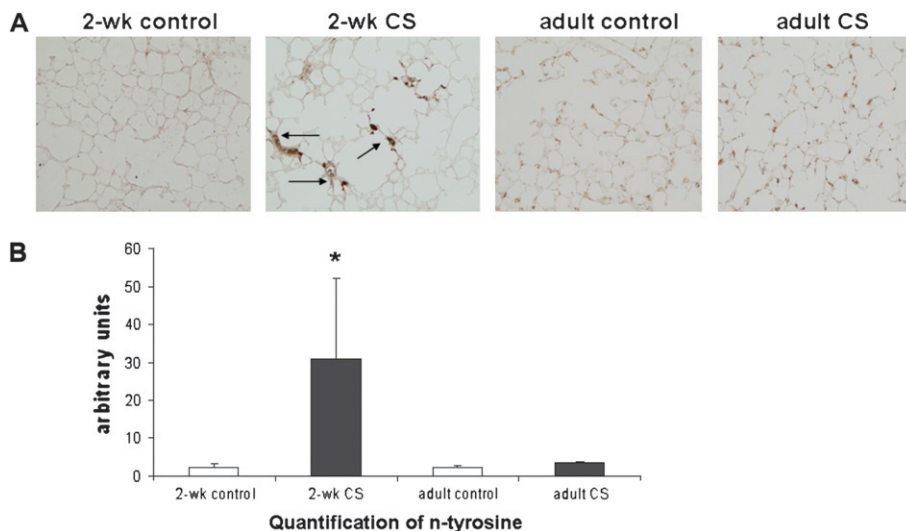
Figure 2. Increased n-tyrosine staining in 2-week-old CS-exposed lung. (*A*) Increased n-tyrosine expression in 2-week-old CS-exposed lung (*black arrows* point to *brown staining*). (*B*) n-Tyrosine staining was significantly increased in 2-week-old CS-exposed lung compared with 2-week-old control lung (*$P < 0.03$ by Wilcoxon rank sum test; 2-week-old CS $n = 6$, 2-week-old control $n = 4$, adult control $n = 3$, and adult smoke $n = 5$, ± SEM).
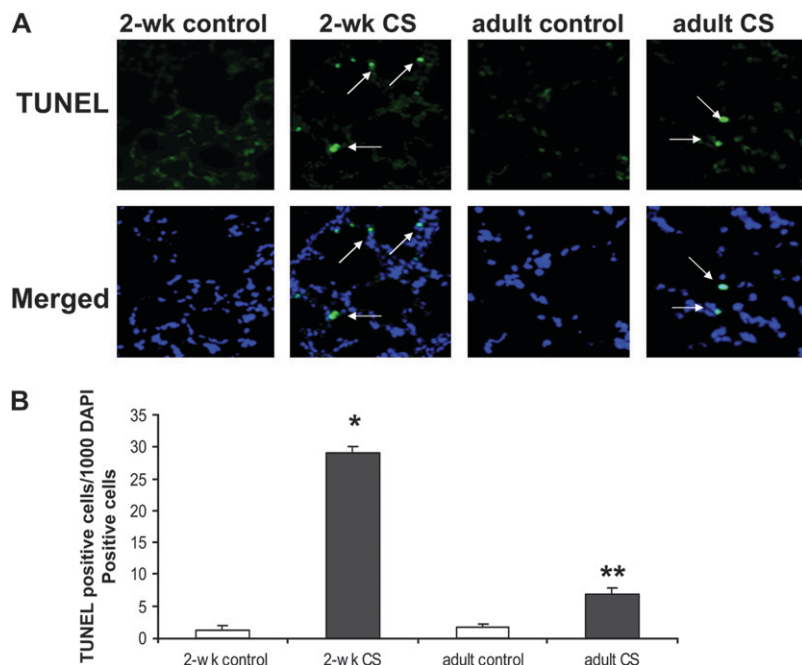
Figure 3. Increased TUNEL staining in 2-week-old CS-exposed lung. (*A*) Increased TUNEL staining found in both 2-week-old and adult CS-exposed lung. (*B*) TUNEL-positive cells/1000 DAPI-–stained cells were significantly greater in 2-week-old CS-exposed lung compared with 2-week-old control, adult control, and adult CS-exposed lung (*$*P < 0.0001$, respectively). Adult CS-exposed lung had significantly greater numbers of TUNEL positive cells than did 2-week-old control and adult control lung (**$**P < 0.0001$ respectively by one-way ANOVA, $n = 3$ for each group, $\pm$ SEM).

with impairment of alveolar growth in the neonatal lung (30). Validation of gene expression profiling by QRT-PCR analysis revealed a 5.2-fold increase in TGF-β2 in CS-exposed lung compared with control lung ($P < 0.01$). To further assess TGF-β signaling in CS-exposed lung, pSMAD2 protein expression was quantified in 2-week-old CS-exposed lung. pSMAD2 staining was significantly increased in 2-week-old lung exposed to CS compared with age-matched control lung (Figure 4, p < 0.01, by Wilcoxon rank sum test). No significant increase in pSMAD2 protein expression was found in adult lung from mice exposed to CS as adults.

Decreased Lung Volume and Decreased Alveolar Number in 8-Week-Old Mice Previously Exposed to Neonatal CS

To determine the long-term effects of neonatal CS exposure on lung development, lung volumes were measured at 8 weeks of age in mice that were exposed to CS in the perinatal period. We found that lung volumes were significantly less in mice previously exposed to CS in the neonatal period compared with age-matched controls ($P < 0.04$) (Table 4). Number of alveoli and radius size were also measured. The number of alveoli in

8-week-old mice previously exposed to neonatal CS was significantly decreased compared with 8-week-old controls ($P < 0.007$). Differences in alveolar radius size, however, did not quite reach significance ($P < 0.07$) (Table 5). Mean linear intercept measurements were also modestly increased in the 8-week-old mice previously exposed to CS in the neonatal period (Figure 5). These data suggest that exposure to CS in the perinatal period can modestly inhibit lung growth.

DISCUSSION

There is abundant evidence that cigarette smoke exposure during perinatal and pediatric life is associated with more respiratory infections and decreased pulmonary function. This study sought to understand the effects of CS exposure on neonatal lung homeostasis during a period of rapid postnatal lung growth using a neonatal murine model. This was addressed using gene expression profiling and histologic and morphologic evaluation of neonatal murine lung exposed to CS during the first 2 weeks of life. We found that perinatal lung is susceptible to the effects of CS exposure. In neonatal mice, daily exposure
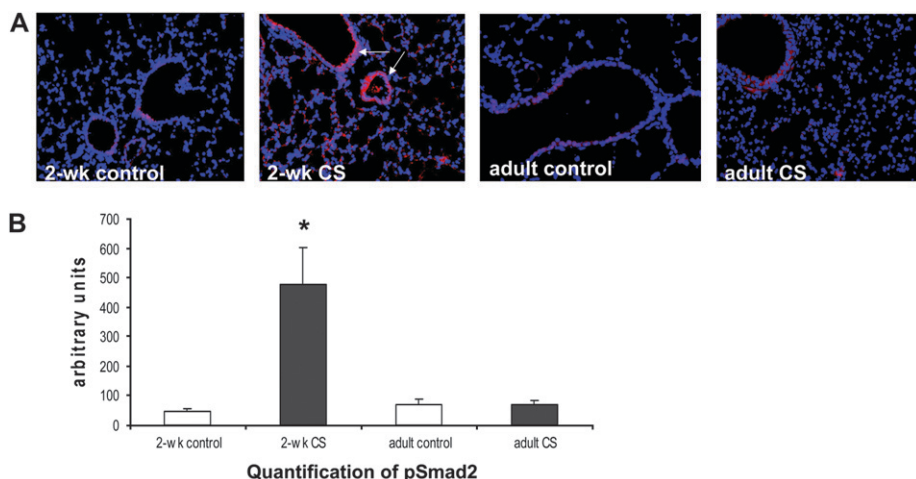
Figure 4. Increased pSMAD2 protein expression in 2-week-old CS-exposed lung. (*A*) pSMAD2 staining was increased in 2-week-old lung exposed to 14 days of CS (*white arrows*). (*B*) pSMAD2 expression was significantly increased in 2-week-old CS-exposed lung compared with 2-week-old control, adult control, and CS-exposed lung. (*$*P < 0.01$, $P < 0.05$, and $P < 0.02$, respectively, by one-way ANOVA; 2-week-old control $n = 5$, 2-week-old CS-exposed $n = 7$, adult control $n = 3$, and adult CS-exposed $n = 5$, $\pm$ SEM).

TABLE 4. EFFECT OF NEONATAL CS EXPOSURE ON LUNG VOLUME

	Body Weight		Lung Volume		Lung Volume/ Body Weight	
	Mean	SD ±	Mean	SD ±	Mean	SD ±
8 wk neonatal cigarette smoke–exposed mice	19.5	2.3	0.22*	0.04	0.011†	0.001
8 wk control mice	18.5	1.6	0.25	0.03	0.014	0.002

Body weight was measured in grams. Lung volume measurements were performed using water displacement as described in MATERIALS AND METHODS. Lung volume values were recorded as a change in weight (grams) with water displacement.

* Statistical differences were found between 8-week-old mice exposed to neonatal cigarette smoke and age-matched control mice for lung volume measurements ($P < 0.04$).

† Statistical differences also were found between 8-week-old mice exposed to neonatal cigarette smoke and age-matched control mice for lung volume/body weight ($P < 0.002$, $n = 11$ for mice exposed to 2 weeks of cigarette smoke and $n = 12$ for age-matched control mice, ± represents SD).

to CS for the first 2 weeks of life inhibited the expression of many genes in the lung that are relevant to the innate immune response. CS exposure also increased oxidative stress, TGF-β signaling, and alveolar cell death in neonatal lung. Furthermore, mice exposed to neonatal CS were found to have mildly impaired lung growth and a modest increase in airspace size. Taken together, these findings highlight a critical period of susceptibility in perinatal life in which exposure to CS can alter expression of genes involved in lung immunity, increase pulmonary oxidative stress and cell death in neonatal lung, and subsequently lead to a modest impairment in lung growth.

Our study was designed to model the effects of CS exposure on neonatal lung. With regard to CS, the duration of time or the level of total particulate matter (TPM) exposure that is required before adverse effects on immune regulation or postnatal lung growth occur is unknown. Due to the close proximity of an infant to its mother, levels of CS to which the infant is exposed may be much higher than that which has been measured from ambient SHS background studies. Decreased TH1 responses were described in neonatal mice exposed to side-stream smoke for more than a month (8). We found that expression of type 1 and type 2 interferon pathway genes were inhibited in neonatal mice exposed to 2 weeks of CS. Future studies should be directed at determining the cumulative amounts of CS exposure that are needed before detrimental effects to the lung and immune system our found. Furthermore, at-risk populations, such as infants and children with pre-existing pulmonary abnormalities and premature infants with bronchopulmonary dysplasia, should be viewed individually, since these groups may require less CS exposure before adverse effects develop.

TABLE 5. EFFECT OF NEONATAL CS EXPOSURE ON LUNG MORPHOMETRY

	Mean Linear Intercept (± SD)	Alveolar Number (± SD)	Alveolar Radius (± SD)
8 wk neonatal cigarette smoke–exposed mice	41.5 ± 1.3*	69.3 ± 4.4†	17.8 ± 1.0
8 wk control mice	37.4 ± 0.6	86.8 ± 6.2	15.8 ± 1.2

* Statistical differences were found between 8-week-old mice exposed to neonatal cigarette smoke and age-matched control mice for mean linear intercept measurements ($P < 0.005$).

† Statistical differences were also found between 8-week-old mice exposed to neonatal cigarette smoke and age-matched control mice for alveolar number ($P < 0.007$, $n = 4$ for mice exposed to 2 weeks of cigarette smoke and $n = 3$ for age-matched control mice, ± represents SD). For alveolar radius size, differences between the two groups did not quite reach statistical significance ($P < 0.07$).
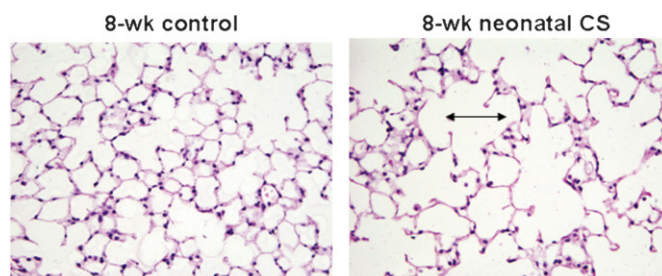
Figure 5. Decreased alveolar numbers and modest increase in mean linear intercept found in 8-week-old mice exposed to neonatal CS.

Our model does not pattern classical adult emphysema, which is slowly progressive in nature and is manifested by cell-induced damage, inflammation, and protease imbalances. Indeed, when we removed neonatal mice from the smoke chamber after a 2-week exposure, we found evidence of necrotic cell death, oxidative stress, and induction of TGF-B signaling in lung tissue, findings consistent with an acute injury. Necrotic cell death in particular is more indicative of an acute injury rather than apoptosis. These lung findings were not found in the adult mice exposed to 2 weeks of CS. The neonatal lung may develop acute changes in response to CS (i.e., 2 wk) because of the rapidly proliferating state of the neonatal lung in contrast to the mature lung.

Recent studies have shown that children raised in areas of high air pollution have significantly reduced lung function compared with children raised in areas of low air pollution (31). Since the perinatal period is an active period of lung growth, human infants may be particularly susceptible to the detrimental effects of environmental pollutants such as CS. In humans, postnatal alveolar growth occurs predominantly during the first 2 years of life, although growth may occur throughout the first decade of life (32). Recently, using aerosol-derived airway morphometry, it was also shown that small airway and alveolar size increased from 6 to 22 years of age, accounting for the change in total lung capacity that occurs with age (33). Since the majority of alveolar growth in the rodent takes place during the first 2 weeks of postnatal life, our model can be useful for studying the susceptibility of the perinatal lung to CS exposure (10, 32, 34). We previously reported that brief exposure to hyperoxia in neonatal mice caused an increase in lung oxidative stress and impaired lung growth resulting in functional changes in the adult animal (11). These findings were consistent with the perinatal period being a time in which the lung is susceptible to the injurious effects of hyperoxia. Our current study suggests that CS exposure may harm the perinatal lung by disrupting lung growth, albeit to a lesser degree then hyperoxia, and may inhibit immune gene expression.

Our findings suggest that the perinatal lung may not be able to respond to CS-induced lung injury as well as the adult lung. We found a significant increase in n-tyrosine staining, a marker for oxidative stress, in neonatal lung exposed to CS. However, by expression profiling we found little induction of stress-responsive antioxidant enzymes involved in glutathione biosynthesis. This is in contrast to adult mice exposed to prolonged CS, in which a marked increase in antioxidant gene expression by pulmonary gene expression profiling was found (35, 36). Taken together, our findings indicate that the neonatal lung may have a decreased ability to respond to increased oxidative stress induced by CS exposure due to an inability to mount a sufficient antioxidant response, or alternatively that longer exposures to CS are needed to induce antioxidant gene expression in the neonatal lung. Neonatal lung exposed to CS also had significantly more alveolar macrophages than age-matched controls. Although not studied in our model, the increase in alveolar macrophages in the CS-

exposed lung may correlate with an increase in metalloprotease release, which may contribute to the increased airspace enlargement found in the adult mice exposed to neonatal CS.

CS exposure is associated with an increased incidence of upper and lower airway infections during early childhood (37, 38). Using gene expression profiling, we found significant inhibition of type 1 and type 2 IFN pathway gene expression in neonatal lung exposed to 2 weeks of CS. This association between CS exposure and inhibition of TH1 response gene expression may occur through a direct inhibitory effect of CS on TH1 gene expression. *In vitro* studies have shown that CS extract can significantly decrease IFN-γ levels in peripheral blood monocytes (6), and that acrolein, a major component of CS, can inhibit IFN-γ transcription in human lymphocytes (39). Alternatively, induction of TGF-β signaling from CS exposure may inhibit TH1 response genes. TGF-β has been shown to inhibit type 2 IFN-γ production from NK cells and impair T cell IFN-γ production (40, 41). Pulmonary genetic profiling in CS-exposed neonatal lung revealed a significant increase in TGF-β2 that was validated by RT-PCR. Increased pSMAD2 expression by immunohistochemistry was also found in neonatal CS-exposed lung consistent with increased TGF-β signaling. In addition to immunosuppression, induction of TGF-β has also been shown to be associated with abnormal alveolar growth (30). Therefore, induction of TGF-β from CS exposure in neonatal lung may alter alveolar lung growth and inhibit pulmonary TH1 gene expression. Future studies will focus on the role of TGF-β signaling on neonatal lung immunity and growth and whether blockade of TGF-β signaling can attenuate the CS-exposed neonatal lung phenotype.

We also found that genes activated by viral dsRNA such as TLR-3, RIG-1, and MDA5 were inhibited in CS-exposed lung. These genes in response to viral invasion can induce type 1 IFN pathway genes. Other genes that act downstream of RIG-1 and can block initiation of translation were also inhibited by CS (*see* Table 2), as was MX1, a GTPase that defends against influenza, and MX2, a related family member. Many of these genes are needed for defense against human respiratory pathogens and impaired expression of these genes may in part explain the increased frequency of lower respiratory illnesses in infants exposed to CS.

In summary, we found that exposure to CS in the neonatal period inhibited type 1 and type 2 IFN pathway gene expression and caused an increase in oxidative stress, alveolar cell death, and TGF-β signaling in neonatal lung. This was followed by a modest impairment in alveolar growth in adult lung previously exposed to CS in the perinatal period. Taken together, our studies support the idea that the perinatal period is a time in which the lung is particularly susceptible to the detrimental effect of CS exposure. Our murine model of CS-induced neonatal lung injury may be useful in investigating pathways that are disrupted or altered in developing lung exposed to CS, and may help with understanding the overall detrimental effects of smoke exposure on the developing lung.

References

1. Joad JP. Smoking and pediatric respiratory health. *Clin Chest Med* 2000; 21:37–46.

2. Jin C, Rossignol AM. Effects of passive smoking on respiratory illness from birth to age eighteen months, in Shanghai, People's Republic of China. *J Pediatr* 1993;123:553–558.

3. Kum-Nji P, Meloy L, Herrod HG. Environmental tobacco smoke exposure: prevalence and mechanisms of causation of infections in children. *Pediatrics* 2006;117:1745–1754.

4. Mitchell EA, Ford RP, Stewart AW, Taylor BJ, Becroft DM, Thompson JM, Scragg R, Hassall IB, Barry DM, Allen EM. Smoking and the sudden infant death syndrome. *Pediatrics* 1993;91:893–896.

5. Sadeghi K, Berger A, Langgartner M, Prusa AR, Hayde M, Herkner K, Pollak A, Spittler A, Forster-Waldl E. Immaturity of infection control in preterm and term newborns is associated with impaired toll-like receptor signaling. *J Infect Dis* 2007;195:296–302.

6. Ouyang Y, Virasch N, Hao P, Aubrey MT, Mukerjee N, Bierer BE, Freed BM. Suppression of human IL-1beta, IL-2, IFN-gamma, and TNF-alpha production by cigarette smoke extracts. *J Allergy Clin Immunol* 2000;106:280–287.

7. Edwards K, Braun KM, Evans G, Sureka AO, Fan S. Mainstream and sidestream cigarette smoke condensates suppress macrophage responsiveness to interferon gamma. *Hum Exp Toxicol* 1999;18:233–240.

8. Phaybouth V, Wang SZ, Hutt JA, McDonald JD, Harrod KS, Barrett EG. Cigarette smoke suppresses Th1 cytokine production and increases RSV expression in a neonatal model. *Am J Physiol Lung Cell Mol Physiol* 2006;290:L222–L231.

9. Burri PH. Structural aspects of postnatal lung development: alveolar formation and growth. *Biol Neonate* 2006;89:313–322.

10. Massaro D, Massaro GD. Invited Review: pulmonary alveoli: formation, the "call for oxygen," and other regulators. *Am J Physiol Lung Cell Mol Physiol* 2002;282:L345–L358.

11. McGrath-Morrow SA, Cho C, Soutiere S, Mitzner W, Tuder R. The effect of neonatal hyperoxia on the lung of p21Waf1/Cip1/Sdi1-deficient mice. *Am J Respir Cell Mol Biol* 2004;30:635–640.

12. Dauger S, Ferkdadji L, Saumon G, Vardon G, Peuchmaur M, Gaultier C, Gallego J. Neonatal exposure to 65% oxygen durably impairs lung architecture and breathing pattern in adult mice. *Chest* 2003;123:530–538.

13. Warner BB, Stuart LA, Papes RA, Wispe JR. Functional and pathological effects of prolonged hyperoxia in neonatal mice. *Am J Physiol* 1998;275:L110–L117.

14. Gauderman WJ, Vora H, McConnell R, Berhane K, Gilliland F, Thomas D, Lurmann F, Avol E, Kunzli N, Jerrett M, *et al.* Effect of exposure to traffic on lung development from 10 to 18 years of age: a cohort study. *Lancet* 2007;369:571–577.

15. Sopori M. Effects of cigarette smoke on the immune system. *Nat Rev Immunol* 2002;2:372–377.

16. Rangasamy T, Cho CY, Thimmulappa RK, Zhen L, Srisuma SS, Kensler TW, Yamamoto M, Petrache I, Tuder RM, Biswal S. Genetic ablation of Nrf2 enhances susceptibility to cigarette smoke-induced emphysema in mice. *J Clin Invest* 2004;114:1248–1259.

17. Scherle W. A simple method for volumetry of organs in quantitative stereology. *Mikroskopie* 1970;26:57–60.

18. MacMicking JD. IFN-inducible GTPases and immunity to intracellular pathogens. *Trends Immunol* 2004;25:601–609.

19. Uthaiah RC, Praefcke GJ, Howard JC, Herrmann C. IIGP1, an interferon-gamma-inducible 47-kDa GTPase of the mouse, showing cooperative enzymatic activity and GTP-dependent multimerization. *J Biol Chem* 2003;278:29336–29343.

20. Akira S, Uematsu S, Takeuchi O. Pathogen recognition and innate immunity. *Cell* 2006;124:783–801.

21. Honda K, Yanai H, Negishi H, Asagiri M, Sato M, Mizutani T, Shimada N, Ohba Y, Takaoka A, Yoshida N, *et al.* IRF-7 is the master regulator of type-I interferon-dependent immune responses. *Nature* 2005;434:772–777.

22. Kato H, Takeuchi O, Sato S, Yoneyama M, Yamamoto M, Matsui K, Uematsu S, Jung A, Kawai T, Ishii KJ, *et al.* Differential roles of MDA5 and RIG-I helicases in the recognition of RNA viruses. *Nature* 2006;441:101–105.

23. Rothenburg S, Deigendesch N, Dittmar K, Koch-Nolte F, Haag F, Lowenhaupt K, Rich A. A PKR-like eukaryotic initiation factor 2alpha kinase from zebrafish contains Z-DNA binding domains instead of dsRNA binding domains. *Proc Natl Acad Sci USA* 2005;102:1602–1607.

24. Hui DJ, Terenzi F, Merrick WC, Sen GC. Mouse p56 blocks a distinct function of eukaryotic initiation factor 3 in translation initiation. *J Biol Chem* 2005;280:3433–3440.

25. Sarkar SN, Kessler SP, Rowe TM, Pandey M, Ghosh A, Elco CP, Hartmann R, Pal S, Sen GC. Natural mutations in a 2′-5′ oligoadenylate synthetase transgene revealed residues essential for enzyme activity. *Biochemistry* 2005;44:6837–6843.

26. Flodstrom-Tullberg M, Hultcrantz M, Stotland A, Maday A, Tsai D, Fine C, Williams B, Silverman R, Sarvetnick N. RNase L and double-stranded RNA-dependent protein kinase exert complementary roles in islet cell defense during coxsackievirus infection. *J Immunol* 2005; 174:1171–1177.

27. Dastur A, Beaudenon S, Kelley M, Krug RM, Huibregtse JM. Herc5, an interferon-induced HECT E3 enzyme, is required for conjugation of ISG15 in human cells. *J Biol Chem* 2006;281:4334–4338.

28. Zhao C, Denison C, Huibregtse JM, Gygi S, Krug RM. Human ISG15 conjugation targets both IFN-induced and constitutively expressed proteins functioning in diverse cellular pathways. *Proc Natl Acad Sci USA* 2005;102:10200–10205.

29. Labrada L, Liang XH, Zheng W, Johnston C, Levine B. Age-dependent resistance to lethal alphavirus encephalitis in mice: analysis of gene expression in the central nervous system and identification of a novel interferon-inducible protective gene, mouse ISG12. *J Virol* 2002;76: 11688–11703.

30. Neptune ER, Frischmeyer PA, Arking DE, Myers L, Bunton TE, Gayraud B, Ramirez F, Sakai LY, Dietz HC. Dysregulation of TGF-beta activation contributes to pathogenesis in Marfan syndrome. *Nat Genet* 2003;33:407–411.

31. Gauderman WJ, Avol E, Gilliland F, Vora H, Thomas D, Berhane K, McConnell R, Kuenzli N, Lurmann F, Rappaport E, *et al.* The effect of air pollution on lung development from 10 to 18 years of age. *N Engl J Med* 2004;351:1057–1067.

32. Thurlbeck WM. Postnatal human lung growth. *Thorax* 1982;37:564–571.

33. Zeman KL, Bennett WD. Growth of the small airways and alveoli from childhood to the adult lung measured by aerosol-derived airway morphometry. *J Appl Physiol* 2006;100:965–971.

34. Wert SE. The lung. In: Polin RA, Fox WW, Abman SH, editors. Fetal and neonatology physiology, 3rd ed. Philadelphia: WB Saunders; 2004.

35. Singh A, Rangasamy T, Thimmulappa RK, Lee H, Osburn WO, Brigelius-Flohe R, Kensler TW, Yamamoto M, Biswal S. Glutathione peroxidase 2, the major cigarette smoke-inducible isoform of GPX in lungs, is regulated by Nrf2. *Am J Respir Cell Mol Biol* 2006;35:639–650.

36. Kensler TW, Wakabayashi N, Biswal S. Cell survival responses to environmental stresses via the Keap1-Nrf2-ARE pathway. *Annu Rev Pharmacol Toxicol* 2007;47:89–116.

37. Mannino DM, Moorman JE, Kingsley B, Rose D, Repace J. Health effects related to environmental tobacco smoke exposure in children in the United States: data from the Third National Health and Nutrition Examination Survey. *Arch Pediatr Adolesc Med* 2001;155: 36–41.

38. Polanska K, Hanke W, Ronchetti R, van den Hazel P, Zuurbier M, Koppe JG, Bartonova A. Environmental tobacco smoke exposure and children's health. *Acta Paediatr Suppl* 2006;95:86–92.

39. Lambert C, McCue J, Portas M, Ouyang Y, Li J, Rosano TG, Lazis A, Freed BM. Acrolein in cigarette smoke inhibits T-cell responses. *J Allergy Clin Immunol* 2005;116:916–922.

40. Laouar Y, Sutterwala FS, Gorelik L, Flavell RA. Transforming growth factor-beta controls T helper type 1 cell development through regulation of natural killer cell interferon-gamma. *Nat Immunol* 2005; 6:600–607.

41. Jarnicki AG, Lysaght J, Todryk S, Mills KH. Suppression of antitumor immunity by IL-10 and TGF-beta-producing T cells infiltrating the growing tumor: influence of tumor environment on the induction of CD4+ and CD8+ regulatory T cells. *J Immunol* 2006;177:896–904.